Inorg. Chem. **2006**, *45*, 5351–5357

Kinetics, Mechanism, and Computational Studies of Rhenium-Catalyzed Desulfurization Reactions of Thiiranes (Thioepoxides)

Abdellatif Ibdah, William S. Jenks,* and James H. Espenson*

Ames Laboratory and Department of Chemistry, Iowa State University, Ames, Iowa 50011-3111

Received December 15, 2005

The oxorhenium(V) dimer $\{MeReO(edt)\}_2$ (**1**; where edt = 1,2-ethanedithiolate) catalyzes S atom transfer from thiiranes to triarylphosphines and triarylarsines. Despite the fact that phosphines are more nucleophilic than arsines, phosphines are less effective because they rapidly convert the dimer catalyst to the much less reactive catalyst $[MeReO(edt)(PAr_3)]$ (**2**). With $AsAr_3$, which does not yield the monomer, the rate law is given by $v = k$[thiirane][**1**], independent of the arsine concentration. The values of k at 25.0 °C in $CDCl_3$ are 5.58 ± 0.08 L mol^{-1} s^{-1} for cyclohexene sulfide and ca. 2 L mol^{-1} s^{-1} for propylene sulfide. The activation parameters for cyclohexene sulfide are $\Delta H^{\ddagger} = 10.0 \pm 0.9$ kcal mol^{-1} and $\Delta S^{\ddagger} = -21 \pm 3$ cal K^{-1} mol^{-1}. Arsine enters the catalytic cycle after the rate-controlling release of alkene, undergoing a reaction with the $Re^{VII}(O)(S)$ intermediate that is so rapid in comparison that it cannot be studied directly. The use of a kinetic competition method provided relative rate constants and a Hammett reaction constant, $\rho = -1.0$. Computations showed that there is little thermodynamic selectivity for arsine attack at O or S of the intermediate. There is, however, a large kinetic selectivity in favor of Ar_3AsS formation: the calculated values of $\Delta H^{\ddagger}$ for attack of $AsAr_3$ at Re═O vs Re═S in $Re^{VII}(O)(S)$ are 23.2 and 1.1 kcal mol^{-1}, respectively.

Introduction

O atom transfer (OAT) reactions have attracted considerable interest, in part because they are prevalent in biology. The oxotransferase enzymes usually contain $Mo^{VI/IV}$, or occasionally $W^{VI/IV}$.[1] Synthetic mimics of the enzymes have been studied, although their catalytic activities are often not high; further, irreversible formation of Mo^{V}_2O causes turnovers to cease. The catalytic cycle occurs between $Mo^{VI}O_2$ and $Mo^{IV}O$.

Certain Re^{V} compounds have proved quite effective at OAT catalysis. The stoichiometry, kinetics, and mechanism of several reactions have now been reported,[2−6] as was recently reviewed.[7,8] Common to all of these systems is repetitive cycling between $L_nRe^{V}O$ and $L_nRe^{VII}(O)_2$ (Scheme 1), where Y is an O atom acceptor such as PAr_3. The corresponding elements of group 6 and 7 catalysts are, of course, isoelectronic when the oxidation states differ by one unit. The catalyst used in the present study is $\{MeReO(edt)\}_2$ (**1**; where edt = 1,2-ethanedithiolate).

Scheme 1. Schematic Mechanism for Re-Catalyzed OAT

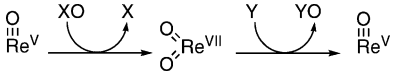

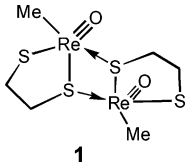

1

S atom transfer (SAT) has been less studied, although S donors such as elemental S,[9,10] thiiranes,[10−13] isothiocyanates RNCS,[13] trisulfides RSSSR,[14] and M═S (M = W,[15] Ti[16]) have found use in synthesis. Thiiranes (episulfides) have been

* To whom correspondence should be addressed. E-mail: wsjenks@iastate.edu (W.S.J.), espenson@iastate.edu (J.H.E.).

(1) Hille, R. *Chem. Rev.* **1996**, *96* (7), 2757−2816.
(2) Huang, R.; Espenson, J. H. *Inorg. Chem.* **2001**, *40* (5), 994−999.
(3) Vasbinder, M. J.; Espenson, J. H. *Organometallics* **2004**, *23* (13), 3355−3358.
(4) Wang, Y.; Espenson, J. H. *Inorg. Chem.* **2002**, *41* (8), 2266−2274.
(5) Wang, Y.; Lente, G.; Espenson, J. H. *Inorg. Chem.* **2002**, *41* (5), 1272−1280.
(6) Wang, Y.; Espenson, J. H. *Org. Lett.* **2000**, *2* (22), 3525−3526.
(7) Espenson, J. H. *Adv. Inorg. Chem.* **2003**, *54*, 157−202.
(8) Espenson, J. H. *Coord. Chem. Rev.* **2005**, *249* (3−4), 329−341.
(9) Taqui Khan, M. M.; Siddiqui, M. R. H. *Inorg. Chem.* **1991**, *30* (5), 1157−1159.
(10) Adam, W.; Bargon, R. M.; Schenk, W. *J. Am. Chem. Soc.* **2003**, *125*, 3871−3876.
(11) Arterburn, J. B.; Perry, M. C. *Tetrahedron Lett.* **1996**, *37*, 7941−7944.
(12) Jacob, J.; Espenson, J. H. *Chem. Commun.* **1999**, *4* (11), 1003−1004.
(13) Hall, K. A.; Mayer, J. M. *J. Am. Chem. Soc.* **1992**, *114*, 10402−10411.
(14) Li, C. J.; Harpp, D. N. *Tetrahedron Lett.* **1993**, *34*, 903−906.
(15) Lupton, D. W.; Taylor, D. K. *Tetrahedron* **2002**, *58*, 4517−4527.
(16) Woo, L. K.; Hays, J. A. *Inorg. Chem.* **1993**, *32* (11), 2228−2289.

10.1021/ic0521426 CCC: $33.50
Published on Web 06/16/2006

prepared from elemental S and from styrene sulfide, which has a weaker C−S bond than the thiiranes obtained. Although $\{Ru^{IV}(edtaH))_2\}_2S_2$ has been reported to catalyze the formation of cyclohexene sulfide from S and cyclohexene,[9] others have been unable to reproduce this result.[10] Rhodium acetate catalyzes sulfinyl transfer from propylene sulfoxide to norbornene and norbornadiene.[17] On the other hand, rhodium acetate does not catalyze the thioepoxidation of cyclooctene or dicyclopentadiene. Even the less exergonic reactions of alkenes and allenes are brought about by this catalyst.[10] The reaction between the M^{IV} complex $[Mo^{IV}(O\text{-}p\text{-}C_6H_6\text{-}X)(S_2C_2\text{-}Me)_2]^-$ and Ph_3AsE (M = W, Mo; E = O, S) forms $AsPh_3$ at a rate of $v = k[M^{IV}][Ph_3AsE]$. The values of k at 25 °C fall in these ranges: for Mo, $(2.3-6.0) \times 10^{-2}$ L mol^{-1} s^{-1} (E = O), $(2.5-7.5) \times 10^{-1}$ L mol^{-1} s^{-1} (E = S); for W, 1.8−9.8 L mol^{-1} s^{-1} (E = O) and 4.1−67 L mol^{-1} s^{-1} (E = S).[18] The higher reactivity of arsine sulfide reflects its weaker As═E bond strength as compared to the oxide: 70[19] and 103[20] kcal mol^{-1}, respectively.

In this study, we have extended the study of SAT to reactions between thiiranes and $PAr_3/AsAr_3$. A dimeric catalyst was chosen because, in earlier studies, dimeric systems had proved ca. 100-fold more effective than monomeric analogues.[21] The general net chemical equation is

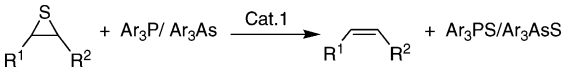

(1)

This system offers the advantage that no uncatalyzed component has been observed. Also, the reaction is thermodynamically favored; values of $\Delta H°$ (and also $\Delta G°$ because, by the symmetry of the reaction, the entropy change will be quite small) are −21 and −7 kcal mol^{-1} for PPh_3 and $AsPh_3$, respectively, from theoretical calculations.[22] A characteristic of catalyst **1** is that reaction 1 proceeds promptly to completion in the case of $AsAr_3$, whereas the PAr_3 reactions are markedly slower, owing to an interfering side reaction, as will be explained.

Experimental Section

Reagents. The Re dimer $\{MeReO(edt)\}_2$ (**1**) was synthesized according to the literature procedure,[23] as were tris(*p*-chlorophenyl)-arsine[24] and tris(*p*-methylphenyl)arsine.[25] All other reagents were obtained from commercial sources and used without further purification except cyclohexene sulfide, which was purified by vacuum distillation. Chloroform-*d* was used as the solvent for kinetics. Benzene-d_6 was used for characterization of the Re^V dimer to compare its ^{1}H and ^{13}C NMR resonances with literature values.[23] The ^{1}H and ^{31}P NMR spectra were recorded at 25 °C by use of a Bruker DRX 400-MHz spectrometer. Triphenylmethane was used as the internal standard in the ^{1}H NMR kinetics experiments.

Kinetics Measurements. The ^{1}H NMR signals of propylene sulfide and cyclohexene sulfide were monitored during the time course of the reaction. The values of the integration were fitted to first-order kinetics, in which Y is the integration area:

$$Y_t = Y_\infty + (Y_0 - Y_\infty)e^{-k_{obs}t}$$

Computational Methods. Computations were carried out using the hybrid density functional B3LYP,[26−29] as implemented in GAMESS.[30] The quoted energies are without temperature correction but contain unscaled zero-point energies. The structures were confirmed as minima or transition states by calculating vibrational frequencies. The structures were optimized with B3LYP using the LANL2DZ ECP[31] for Re, augmented with 2f[32] polarization functions. Pople-style basis sets were used for the lighter elements: 6-31+G(d) for S and O atoms and 6-31G(d) for other atoms.[33−35] The zero-point energies were calculated with the same basis sets and level of theory. Energies were refined with single-point calculations, also done with B3LYP, but using larger basis sets: G3Large for S, As, and P,[36,37] 6-311+G(2d) for O and N,[34,38] and 6-31G(d) for C and H, along with the original basis set for Re.

Results

Preliminary Experiments with Phosphines. NMR spectroscopy was used in the experimental studies. First, ^{31}P NMR spectroscopy demonstrated that Ph_3PS is the only P-containing product formed from propylene sulfide (Figure 1). The timed decrease of the propylene sulfide resonances and the concomitant growth of the propylene resonances are shown in Figure 2 and seem to follow first-order kinetics, although only single experiments were run.

Without extensive study, the rate appears to be independent of the *concentration* of PPh_3, in that its concentration decreased by 70% during the experiment, evidently without

(17) Kendall, J. D.; Simpkins, N. S. *Synlett* **1998**, 391−392.
(18) Wang, J.-J.; Kryatova, O. P.; Rybak-Akimova, E. V.; Holm, R. H. *Inorg. Chem.* **2004**, *43*, 8092−8101.
(19) Capps, K. B.; Wixmerten, B.; Bauer, A.; Hoff, C. D. *Inorg. Chem.* **1998**, *37*, 2861−2864.
(20) Barnes, D. S.; Burkinshaw, P. M.; Mortimer, C. T. *Thermochem. Acta* **1998**, *131*, 107−113.
(21) Koshino, N.; Espenson, J. H. *Inorg. Chem.* **2003**, *42* (18), 5735−5742.
(22) Ibdah, A.; Espenson, J. H.; Jenks, W. S. *Inorg. Chem.* **2005**, *44* (23), 8426−8432.
(23) Espenson, J. H.; Shan, X.; Wang, Y.; Huang, R.; Lahti, D. W.; Dixon, J.; Lente, G.; Ellern, A.; Guzei, I. A. *Inorg. Chem.* **2002**, *41* (9), 2583−2591.
(24) de Ketelaere, R. F.; Delbeke, F. T.; Van der Kelen, G. P. *J. Organomet. Chem.* **1971**, *28*, 217−223.
(25) McCortney, B. A.; Jacobson, B. M.; Vreeke, M.; Lewis, E. S. *J. Am. Chem. Soc.* **1990**, *112*, 3554−3559.
(26) Becke, A. D. *Phys. Rev. A* **1988**, *38* (6), 3098−3100.
(27) Becke, A. D. *J. Chem. Phys.* **1993**, *98* (7), 5648−5652.
(28) Stephens, P. J.; Devlin, F. J.; Chabalowski, C. F.; Frisch, M. J. *J. Phys. Chem.* **1994**, *98* (45), 11623−11627.
(29) Hertwig, R. H.; Koch, W. *Chem. Phys. Lett.* **1997**, *268* (5−6), 345−351.
(30) Schmidt, M. W.; Baldridge, K. K.; Boatz, J. A.; Elbert, S. T.; Gordon, M. S.; Jensen, J. H.; Koseki, S.; Matsunaga, N.; Nguyen, N.; Su, S. J.; Windus, T. L.; Dupuis, M.; Montgomery, J. A. *J. Comput. Chem.* **1993**, *14*, 1347−1363.
(31) Hay, P. J.; Wadt, W. R. *J. Chem. Phys.* **1985**, *82* (1), 299−310.
(32) Gisdakis, P.; Antonczak, S.; Roesch, N. *Organometallics* **1999**, *18* (24), 5044−5056.
(33) Hariharan, P. C.; Pople, J. A. *Theor. Chim. Acta* **1973**, *28* (3), 213−222.
(34) Clark, T.; Chandrasekhar, J.; Spitznagel, G. W.; Schleyer, P. v. R. *J. Comput. Chem.* **1983**, *4* (3), 294−301.
(35) Hehre, W. J.; Ditchfield, R.; Pople, J. A. *J. Chem. Phys.* **1972**, *56*, 2257−2261.
(36) Curtiss, L. A.; Raghavachari, K.; Redfern, P. C.; Rassolov, V.; Pople, J. A. *J. Chem. Phys.* **1998**, *109* (18), 7764−7776.
(37) Curtiss, L. A.; Redfern, P. C.; Rassolov, V.; Kedziora, G.; Pople, J. A. *J. Chem. Phys.* **2001**, *114* (21), 9287−9295.
(38) Krishnan, R.; Binkley, J. S.; Seeger, R.; Pople, J. A. *J. Chem. Phys.* **1980**, *72*, 650−654.

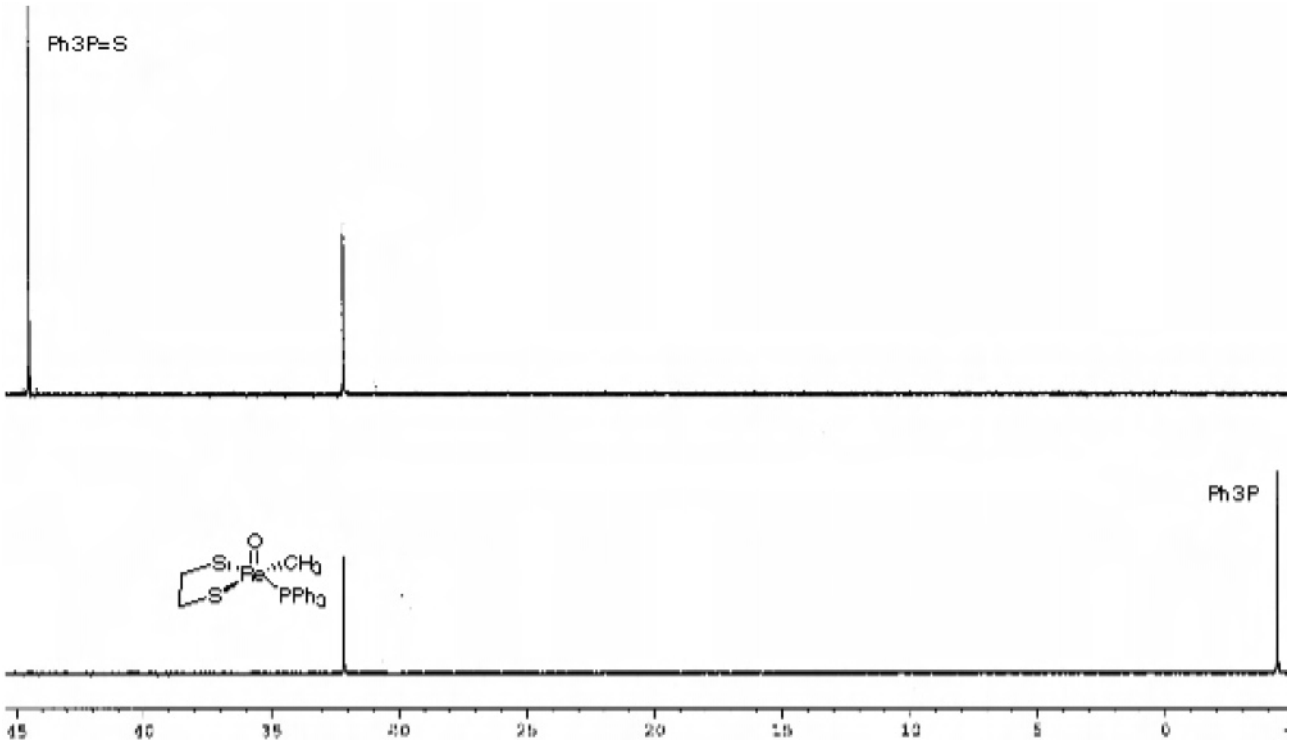

Figure 1. ^{31}P NMR spectrum before (below) and after (above) completion (5 h) of a reaction between 250 mmol L^{-1} PrS, 60 mmol L^{-1} PPh_3, and 10 mmol L^{-1} **1**. The sole resonance is that of Ph_3PS at δ 44 ppm in $CDCl_3$. The signal of **2**, the monomeric product from **1**, is clearly evident in both spectra.

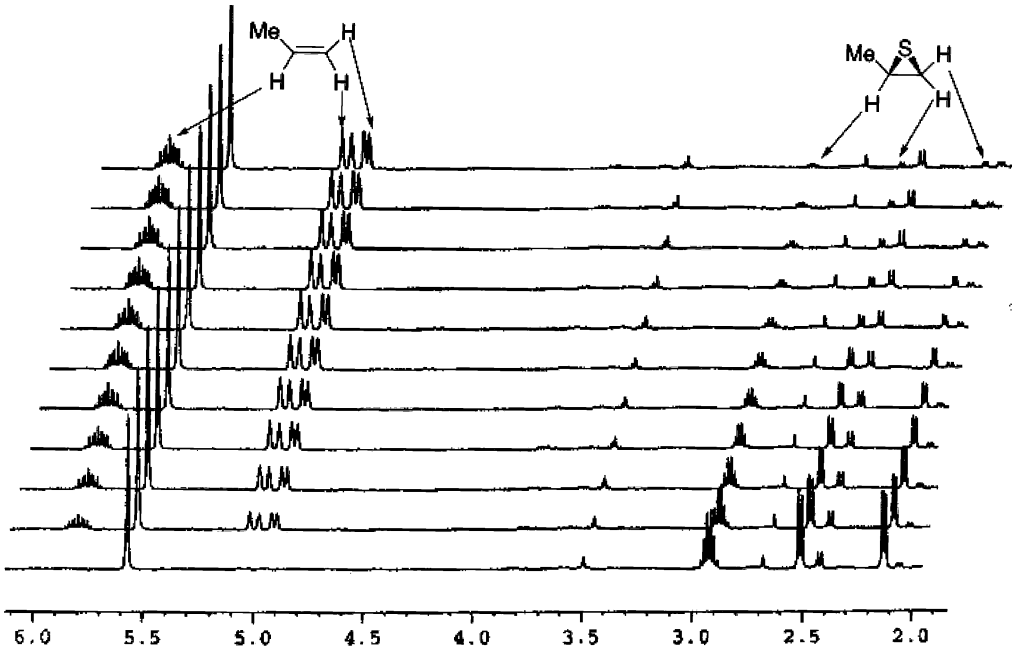

Figure 2. Stacked ^{1}H NMR spectra taken during the reaction of 184 mmol L^{-1} PPh_3, 128 mmol L^{-1} PrS, and 9.0 mmol L^{-1} of **1**. Data were taken at 25 °C in $CDCl_3$ at intervals of 30 min.

effect. It is surprising, therefore, that the rate constant does depend on the *identity* of the group X of $P(C_6H_4$-*p*-$X)_3$ (X = MeO, H, Cl) as shown in Figure 3. This and related issues will be taken up in the Discussion section.

The added catalyst was **1**, but it is rapidly converted to [MeReO(edt)(PAr_3)] (**2**), as shown in Scheme 2.[39] The rate law for this transformation is given in eq 3.

$$-\mathrm{d}[\mathbf{1}]/\mathrm{d}t = \{k_a[PPh_3] + k_b[PPh_3]^2\}[\mathbf{1}] \qquad (2)$$

The rate constants at 25 °C are $k_a = 0.83$ L mol^{-1} s^{-1} and $k_b = 23.7$ L^2 mol^{-2} s^{-1}.[23] Therefore, at 0.184 mol L^{-1} PPh_3, as in Figures 2 and 3, $k_{obs} = 0.96$ s^{-1} or $t_{1/2} = 0.73$ s. Because monomerization is so rapid, the data in these experiments actually pertain to catalysis of reaction 1 by **2**.

Experiments with Arsines. Scheme 2 indicates that **1** is stable with respect to monomerization by arsines, even over

(39) Lente, G.; Jacob, J.; Guzei, I. A.; Espenson, J. H. *Inorg. React. Mech. (Amsterdam)* **2000**, *2* (3), 169−177.

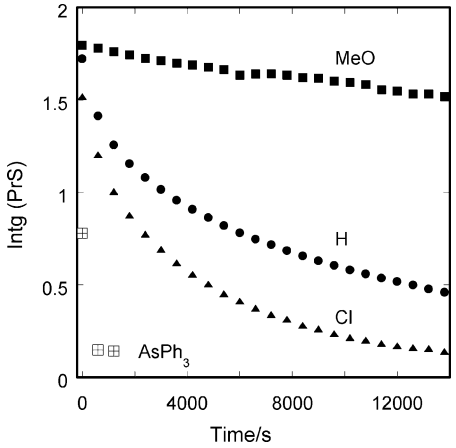

Figure 3. Time course experiments of the integrated PrS resonance against time with three PAr_3 compounds and the much more rapidly reacting $AsPh_3$.

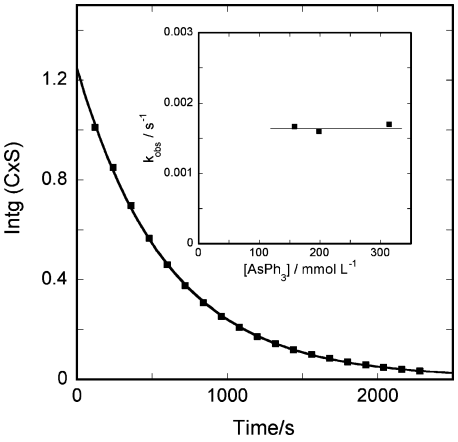

Figure 4. First-order fitting of the intensity of the δ 3.15 ppm ^{1}H NMR resonance of CxS in an experiment with 92 mmol L^{-1} CxS, 158 mmol L^{-1} $AsPh_3$, and 0.32 mmol L^{-1} **1** at 25 °C in CD_3CN. Inset: Plot of k_{obs} against [$AsPh_3$], showing its lack of effect.

Scheme 2. Monomerization of **1** Occurring with Phosphines but Not Arsines

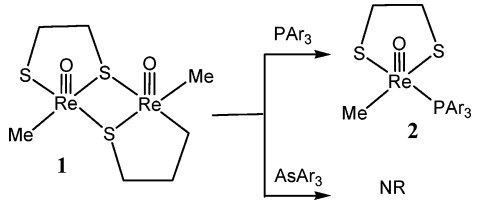

extended reaction times. Indeed, in our experience in the area, no [MeReO(dithiolato)($AsAr_3$)] species has been detected, let alone isolated. We surmise that the failure of arsines to react with **1** manifests equilibrium issues: the arsine is too sterically demanding and too weak a Lewis base.

For these reasons, subsequent studies used only $AsAr_3$ as the S atom acceptors. Also, most of the subsequently reported kinetics studies were carried out with CxS because PrS is rather volatile. The arsine reaction is first-order with respect to the thiirane concentration (Figure 4), independent of [$AsPh_3$] over the range 150−320 mmol L^{-1} (inset to Figure 4), and first-order with respect to the catalyst concentration (see Figure 5 and eq 3). The values of k are 5.58 ± 0.08 L mol^{-1} s^{-1} at 25.0 °C in $CDCl_3$ for CxS and ca. 2 L mol^{-1} s^{-1} for PrS. Likewise, k is independent of the identity of the

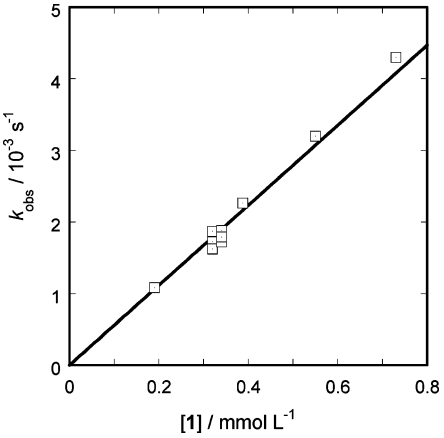

Figure 5. Plot of k_{obs} against the catalyst concentration in a series of experiments with 92 mmol L^{-1} CxS and 65−314 mmol L^{-1} $AsPh_3$.

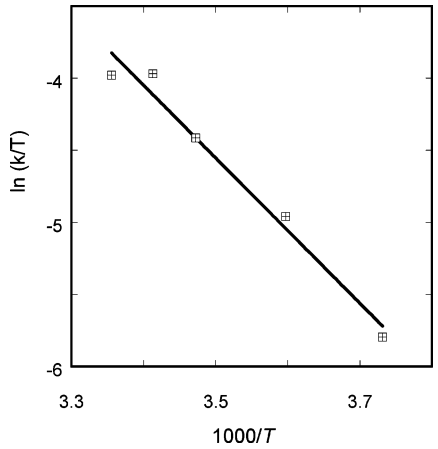

Figure 6. Plot of ln(k/T) vs 1/T according to eq 4, where the second-order rate constant, k, of eq 3 applies to the reaction between cyclohexene sulfide and triphenylarsine, catalyzed by **1**.

aryl ring substituent as well: for CxS with $As(C_6H_4X)_3$, k = 5.7 ± 0.5 (X = Me) and 5.5 ± 0.1 (X = Cl) L mol^{-1} s^{-1}.

$$-\mathrm{d}[\mathrm{C} \times \mathrm{S}]/\mathrm{d}t = k[\mathrm{C} \times \mathrm{S}][\mathbf{1}] \qquad (3)$$

Activation Parameters. The second-order rate constant for the CxS reaction, as defined in eq 3, was determined at the additional temperatures of −5.0, 5.0, 15.0, 20.0, and 25.0 °C. The data were fit by the transition-state theory equation

$$\ln(k/T) = \ln(k_B/h) + \Delta S^{\ddagger}/R - \Delta H^{\ddagger}/RT \qquad (4)$$

Figure 6 displays the plot of ln(k/T) vs 1/T, from which these values were obtained: $\Delta H^{\ddagger}$ = 10.0 ± 0.9 kcal mol^{-1} and $\Delta S^{\ddagger}$ = −21 ± 3 cal K^{-1} mol^{-1}.

Competition between Arsines. Because k is independent of the arsine identity, arsine enters the catalytic cycle following the rate-controlling step. Kinetics data for the step involving $AsAr_3$ must therefore be obtained by competition methods, and then only the relative values of the rate constants for this reaction stage can be evaluated. With the use of two arsines in a given experiment, the ratio of rates,

in terms of shorthand notation, X = $As(ArX)_3$, Y = $As(ArY)_3$, XS = $(ArX)_3AsS$, and YS = $(ArY)_3AsS$, is

$$\frac{-dX/dt}{-dY/dt} = \frac{dXS/dt}{dYS/dt} = \frac{dX}{dY} = \frac{k_X}{k_Y}\frac{X}{Y} \quad (5)$$

Integration affords an expression for the rate constant ratio:

$$\ln X|_0^t = \frac{k_X}{k_Y} \times \ln Y|_0^t \Rightarrow \frac{k_X}{k_Y} = \frac{\ln\left(\frac{X_t}{X_0}\right)}{\ln\left(\frac{Y_t}{Y_0}\right)} = \frac{\ln\left(\frac{X_0 - XS_t}{X_0}\right)}{\ln\left(\frac{Y_0 - YS_t}{Y_0}\right)} \quad (6)$$

The concentration of each arsine sulfide was determined by integration of the ^1H NMR spectrum during the reaction. The rate constant ratios, k_X/k_Y, were normalized relative to $AsPh_3$ (k = 1.00). The ratios and the Hammett substituent constants are as follows:

$As(C_6H_4X)_3$	k_X/k_H	σ
$As(C_6H_4$-*p*-$Me)_3$	2.87	−0.17
$AsPh_3$	1.00 (rel.)	0
$As(C_6H_4$-*p*-$Cl)_3$	0.18	0.23

Computational Studies: Background. Mixed thio−oxo compounds have been reported for W^{VI} and Mo^{VI}.[18,40,41] Whereas $W^{VI}(O)_2$ does not perform clean OAT,[42] $W^{VI}(S)_2$ leads to rapid SAT with PPh_3.[43] The relevant bond strengths are 138−160 kcal mol^{-1} for W═O and 82−92 kcal mol^{-1} for W═S.[44] Even though the P═O bond is stronger than the P═S bond (128.4[45] vs 88[19] kcal mol^{-1}), PPh_3 reacts faster with the thio group than with the oxo. Similarly, SAT is observed for a W(O)(S) catalyst, despite thermodynamic preference for the oxo transfer.[46]

Qualitative representations of the π and π^* levels of W^{VI}═S and W^{VI}═O in $W^{VI}(O)(S)$ have been reported,[46] according to which the energy of the W═O π orbital lies well below the energy of the frontier orbitals. Further, the very high energy of the W═O π^* orbital limits nucleophilic attack on the oxo group. The frontier orbitals [highest occupied molecular orbital (HOMO) and lowest unoccupied molecular orbital (LUMO)] of $W^{VI}(O)(S)$ are the π and π^* orbitals of the W═S bond, such that the LUMO (W═S π^*) lies considerably lower in energy than W═O π^*. It is on these terms that one can understand kinetic control favoring SAT over OAT.[46]

In the case of Re catalysis, the experimental finding is that SAT provides the exclusive pathway. Calculations of the energetics of the Re═E bonds in $[MeRe^{VII}(edt)(O)(S)]$, the monomeric analogue of the putative dirhenium intermediate, gave respective gas-phase Re═S and Re═O bond strengths of 84 and 118 kcal mol^{-1}. Given the Ph_3P═O and Ph_3P═S bond strengths, OAT to PPh_3 is therefore thermodynamically favored over SAT by 6 kcal mol^{-1}. This result shows that a prediction from thermodynamics seemingly contradicts the experimental reaction stoichiometry. In the following section, computational results are presented that address the apparent kinetic preference for SAT over OAT.

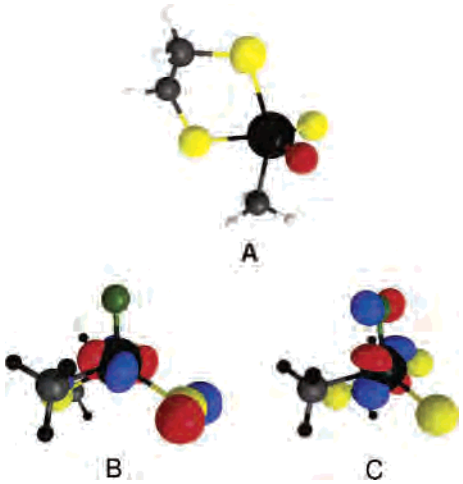

Figure 7. Calculated structure for **A** illustrating the distorted trigonal-bipyramidal shape and the π^* orbitals for ReS (**B**) and ReO (**C**). The orientation of the molecule is the same for **B** and **C** but rotated relative to **A**. O atoms are shown in green for **B** and **C** for clarity of the orbitals.

Computational Studies: Results. The proposed transition state for the rate-controlling step involves alkene release from a thiirane−Re complex; in skeleton form, the net result is represented by eq 7. Computations afford $\Delta H_2^{\ddagger}$ = 6.9 kcal mol^{-1} of cyclohexene released.

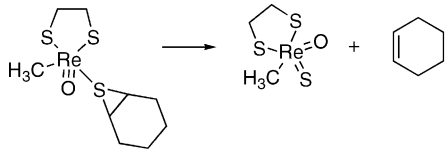

(7)

The next reaction in need of examination is the one in which triphenylarsine attacks the oxo−thio−Re^{VII} intermediate. Although not rate-controlling, this step is where the choice of OAT vs SAT is made for a given catalytic cycle. Here, PMe_3 and $[MeRe^{VII}(edt)(O)(S)]$ (**A**) were used as models for $AsPh_3$ and for the actually dimeric oxo−thio−Re^{VII} intermediate. Will phosphine form Ph_3PO or Ph_3PS upon reaction with the $Re^{VII}(O)(S)$ species? First, calculations show only a modest thermodynamic preference for one mode of reaction over the other: $\Delta H°$ = −31 and −27 kcal mol^{-1} for PMe_3 attack at O and S, respectively.

The calculated structure of **A** is a distorted trigonal bipyramid (Figure 7). Transition-state geometries for phosphine attack on $[MeRe^{VII}(edt)(O)(S)]$ were first optimized with the same basis sets as those used for the optimizations. Transition-state energies for phosphine attack on $[MeRe^{VII}(edt)(O)(S)]$ were then calculated with larger basis sets, as

(40) Thapper, A.; Donahue, J. P.; Musgrave, K. B.; Willer, M. W.; Nordlander, E.; Hedman, B.; Hodgson, K. O.; Holm, R. H. *Inorg. Chem.* **1999**, *38*, 4104−4114.
(41) Young, C. G.; Laughlin, L. J.; Colmanet, S.; Scrofani, S. D. B. *Inorg. Chem.* **1996**, *35*, 5368−5377.
(42) Eagle, A. A.; Tiekink, E. R. T.; Young, C. G. *Inorg. Chem.* **1997**, *36*, 6315−6322.
(43) Eagle, A. A.; Gable, R. W.; Thomas, S.; Sproules, S. A.; Young, C. G. *Polyhedron* **2004**, *23*, 385−394.
(44) Bryan, J. C.; Mayer, J. M. *J. Am. Chem. Soc.* **1990**, *112*, 2298−2308.
(45) Bedford, A. F.; Mortimer, C. T. *J. Chem. Soc.* **1960**, 1622−1625.
(46) Eagle, A. A.; Tiekink, E. R. T.; George, G. N.; Young, C. G. *Inorg. Chem.* **2001**, *40*, 4563−4573.

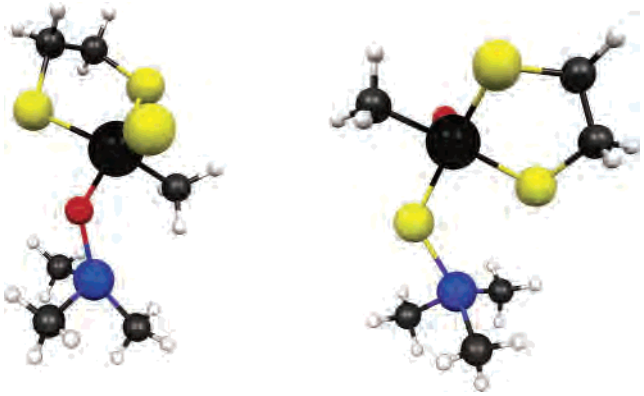

Figure 8. Transition states for PMe_3 attack of **A** at O or S. The molecule is rotated to show the P−O−Re and P−S−Re angles, which are 124° and 139°, respectively.

outlined above. The transition-state geometries are illustrated in Figure 8, and some key geometric parameters are given in the Supporting Information, along with the coordinates. It was verified by means of intrinsic reaction coordinate calculations that the located transition states do "connect" the starting material and reaction products correctly. Notably, the attack of the phosphine is *not* a prototypical "backside attack" of an archetypal S_N2 reaction, despite the steric accessibility. Rather, the bent geometry of attack (Re−E−P) indicates that interaction with the Re═E π system is involved in the reaction. The transition-state energies afford calculated activation enthalpies of $\Delta H^{\ddagger} = 17.8$ kcal mol^{-1} and a remarkably low 1 kcal mol^{-1} for attack at O and S, respectively. The magnitude of this difference, despite the approximations introduced by the use of simplified chemical models and the neglect of solvent interactions, provides a sufficient rationale for the kinetic preference of SAT over OAT. In support of this notion, the molecular orbital pictures of the Re═E π* orbitals are shown as **B** (E = S) and **C** (E = O). The energy of the Re═O π* orbital is 19 kcal mol^{-1} higher than that of the analogous Re═S orbital.

Discussion

Proposed Chemical Mechanism. The kinetics and computational data allow the formulation of a mechanism that accommodates all of the findings. It is presented in Scheme 3. We envisage that the first stage is thiirane coordination to one Re atom of **1** concomitant with the release of one S → Re coordinate bond. In that manner, an optimal five-coordinate geometry about Re^{V} is preserved in a **1**−thiirane intermediate, designated **3**, that remains at an undetectable concentration. The subsequent and rate-controlling step is the irreversible release of alkene. The steady-state rate law from this scheme is

$$v = \frac{k_1 k_2}{k_{-1} + k_2}[\mathbf{1}][\text{thiirane}] \cong K_1 k_2 [\mathbf{1}][\text{thiirane}] \qquad (8)$$

On the basis of the chemical arguments given above, the rate constant for thiirane release will greatly exceed alkene formation, or $k_{-1} \gg k_2$. Thus, the experimental rate constant $k = K_1 k_2$. We propose that the two components of K_1, which

Scheme 3. Proposed Mechanism for Reaction 1

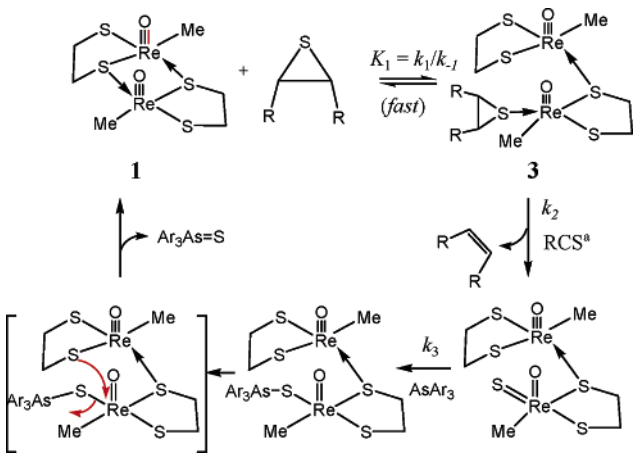

[a] Rate-controlling step.

is ≪1, are a small, endothermic value of ΔH_1° and a substantially negative value of ΔS_1°, the latter because two molecules unite to become one in this rapid equilibrium. The experimental values $\Delta H^{\ddagger} = \Delta H_1^{\circ} + \Delta H_2^{\ddagger}$ and $\Delta S^{\ddagger} = \Delta S_1^{\circ} + \Delta S_2^{\ddagger}$ can be analyzed in these terms. With the computed value $\Delta H_2^{\ddagger} = 6.9$ kcal mol^{-1} and $\Delta H^{\ddagger} = 10.0$ kcal mol^{-1}, $\Delta H_1^{\circ} =$ ca. 3 kcal mol^{-1}. This value, albeit approximate, is consistent with the proposal made. Offsetting the postulated negative value of ΔS_1° is the presumably opposing and smaller effect of $\Delta S_2^{\ddagger}$, which we anticipate to be positive because it represents alkene dissociation. Evidently, that event is not far advanced in the transition state because the experimental value of $\Delta S^{\ddagger}$ is negative. The values of $\Delta H^{\ddagger}$ and $\Delta H_2^{\ddagger}$ are substantially larger than the computationally derived value of $\Delta H_3^{\ddagger}$ for the step in which arsine attacks at the thio group, 1.1 kcal mol^{-1}. The small activation enthalpy calculated for the k_3 step, therefore, makes it clear why the alkene release step, rather than the arsine attack, is rate-controlling; i.e., arsine attacks the $Re^{VII}(O)(S)$ intermediate in a reaction with a rate constant much higher than that of the preceding step. A factor of 3 separates the values of k for CxS and PrS, corresponding to $\Delta\Delta G^{\ddagger} = 0.5$ kcal mol^{-1}. The difference is too small to comment upon, particularly because k represents the composite $K_1 k_2$.

Relative values of k_3 were obtained by the competition method described earlier. The analysis of these data by Hammett's method gives a reaction constant $\rho = -1.03 \pm 0.07$, as shown in Figure 9. Such a large, negative value supports the designation of this step as being nucleophilic attack on S. The next-formed intermediate is a Ph_3AsS complex of Re^{V}, which releases this weak Lewis base rapidly as the S → Re bond is restored.

Comparing PAr_3 and $AsAr_3$. The rate constant for the Figure 4 experiment with $AsPh_3$ corresponds to $t_{1/2} = \ln 2/(5.85\ \text{L mol}^{-1}\ \text{s}^{-1} \times 3.2 \times 10^{-4}\ \text{mol L}^{-1})$, or 388 s. On the basis of Scheme 3, a reaction with PPh_3 instead would have the same [PPh_3]-independent $t_{1/2}$ were it not for the rapid monomerization of **1**. This is entirely hypothetical, of course, because monomerization is so much faster. This analysis presupposes that the overall rates of the arsine and phosphine reactions would be identical because they enter

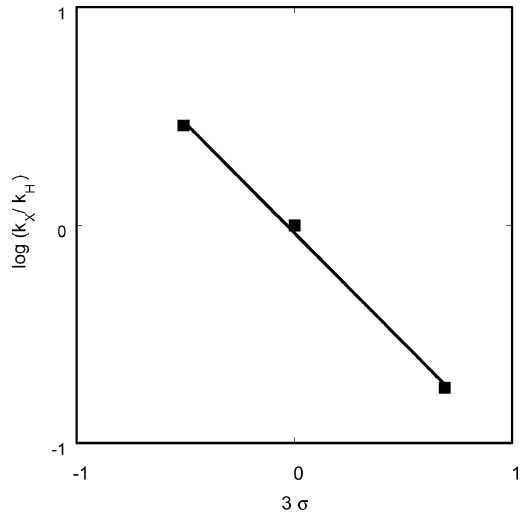

Figure 9. Hammett analysis of the relative rate constants for the stage at which $AsAr_3$ attacks the $Re^{VII}(O)(S)$ intermediate, designated as k_3 in Scheme 3.

the sequence after the rate-controlling step. There is actually little doubt, however, that $k_{3,P} > k_{3,As}$, given the comparative nucleophilicities of the two.

Catalysis by 2. The data are limited to the information shown in Figure 2, so a full description of the kinetics and mechanism cannot be given. The rates are sensitive to the identity of the aryl ring substituent in $P(C_6H_4\text{-}p\text{-}X)_3$, declining in the order X = Cl > H > MeO, opposite to the order of the Lewis basicities. This is a strong indication that PAr_3 must first be displaced from **2** to sustain catalytic action at each cycle.

A close analogue of **2**, [MeReO(mtp)(PAr_3)], where $mtpH_2$ is 2-(mercaptomethyl)thiophenol, catalyzes OAT from pyridine *N*-oxides to triphenylphosphine.[4] The rate is inversely proportional to [PPh_3]. The rate constants follow the same trend with aryl ring substituents: Cl > H > MeO, etc., with a reaction constant $\rho = +1.03$.[4] This indicates that the initial step is phosphine displacement in an uphill equilibrium and suggests that phosphine displacement from **2** is a feature of the SAT mechanism for this catalyst.

$$[MeReO(mtp)(PAr_3)] + PyO = [MeReO(mtp)(OPy)] + PAr_3 \quad (9)$$

In the later and rapid k_3 reaction, the relative rate constants from competition experiments for SAT from CxS to $AsAr_3$ afford the reaction constant $\rho = -1.0$ (Figure 9). In comparison, OAT from PyO to PAr_3 is characterized by $\rho = -0.70$.[4] Negative reaction constants in both instances confirm the nucleophilic nature of the k_3 step in Scheme 3 for SAT from thiiranes and its analogue for OAT from pyridine *N*-oxides.

Acknowledgment. This work was supported by the U.S. Department of Energy under Contract W-7405-Eng-82 and by a SPRIG grant from Iowa State University to W.S.J. Computational time was provided by the NCSA (National Center for Supercomputing Applications) through the use of NCSA's IBM P690 system.

Supporting Information Available: Stacked ^1H NMR spectra and MacMolPlot drawings (Figures S1−S3) and tables of kinetics data and of coordinates and absolute energies (Tables S1−S4). This material is available free of charge via the Internet at http://pubs.acs.org.

IC0521426